JOURNAL OF MATERIALS SCIENCE 24 (1989) 1623–1628

Improvement of creep-rupture properties of wrought cobalt-based HS-21 alloys at high temperatures

M. TANAKA, H. IIZUKA, F. ASHIHARA
Department of Mechanical Engineering for Production, Mining College, Akita University, 1-1, Tegatagakuen-cho, Akita 010, Japan

The improvement of creep-rupture properties by serrated grain boundaries is investigated using wrought cobalt-based HS-21 alloys in the temperature range 816 to 1038° C (1500 to 1900° F). Serrated grain-boundaries are produced in the early stage of the grain-boundary reaction (GBR) by a heat treatment. Specimens with serrated grain boundaries have superior creep-rupture properties compared with those with normal straight grain boundaries. The rupture lives of specimens with serrated grain boundaries are more than twice as long as those of specimens with straight grain boundaries. The rupture elongation is considerably improved by serrated grain boundaries especially at lower temperatures. A ductile grain-boundary fracture is observed in specimens with serrated grain boundaries, while brittle grain boundary facets prevail in specimens with straight grain boundaries.

1. Introduction

Cobalt-based superalloys have excellent corrosion resistance and thermal fatigue strength, and are comparable in strength to nickel-based superalloys at temperatures above about 900° C [1, 2]. Most of the cobalt-based superalloys are strengthened by the formation of carbides which are more stable than in nickel-based superalloys, where they tend to dissolve at high temperatures.

In cobalt-based HS-21 alloys which contain relatively large amounts of carbon (about 0.25 wt %), the grain-boundary reaction (GBR) occurs readily during a heat treatment [3–7]. Hoffman and Robards [4] have reported that an improvement in rupture life of HS-21 gas-turbine blade at 816° C (1500° F) was possibly associated with grain-boundary reaction precipitates (a lamellar microstructure) produced by heat treatments. The present authors [8] revealed that a large strengthening of HS-21 alloys was achieved when serrated grain boundaries with a small amount of the grain-boundary reaction (about 7% in area fraction) were accompanied by large amounts of matrix precipitates which precipitated during creep. However, a large extent of grain-boundary reaction degraded the creep-rupture strength of the alloys at 816° C, while it largely improved the creep ductility. Similar results were reported on austenitic 21Cr–4Ni–9Mn heat-resisting steels [9]. Therefore, it is necessary in order to improve creep-rupture properties of HS-21 alloys to develop serrated grain boundaries accompanied by large amounts of matrix precipitates while keeping the extent of the grain-boundary reaction small. However, the effectiveness of strengthening by serrated grain boundaries was not known in these alloys at temperatures much higher than 816° C. In this study, the improvement of creep-rupture properties by grain-boundary reaction precipitates was investigated using wrought HS-21 alloys in the temperature range 816 to 1038° C (1500 to 1900° F).

2. Experimental procedure

Table I shows the chemical composition of cobalt-based HS-21 alloys used in this study. A 30 kg ingot of cast HS-21 alloy was hot-forged to bars with 16 mm diameter at 1150° C. Specimens for microscopic observations and creep experiments were cut from these bars and heat treated. Fig. 1 shows the microstructures of the specimens. Specimens with serrated grain boundaries (alloy S) were obtained by furnace cooling to 1050° C and subsequent water quenching after solution heating for 1 h at 1250° C. Specimens with normal straight grain boundaries (alloy N) were solution heated for 1 h at 1250° C and then water quenched. Fig. 2 shows the transmission electron micrographs of these specimens. Nodules containing rod-like precipitates are formed on grain boundaries by the grain-boundary reaction in alloy S (Fig. 2b), while no precipitates occur in alloy N (Fig. 2a). The selected-area diffraction (SAD) pattern of Fig. 2b shows that the rod-like precipitates in nodules are $M_{23}C_6$-type

TABLE I Chemical composition of cobalt-based alloys used (wt %)

Alloy	C	Cr	Ni	Mo	Mn	Fe	Si	P	S	B	Co
HS-21	0.27	26.71	2.37	5.42	0.64	0.09	0.59	< 0.005	0.007	0.003	Balance

0022–2461/89 $03.00 + .12

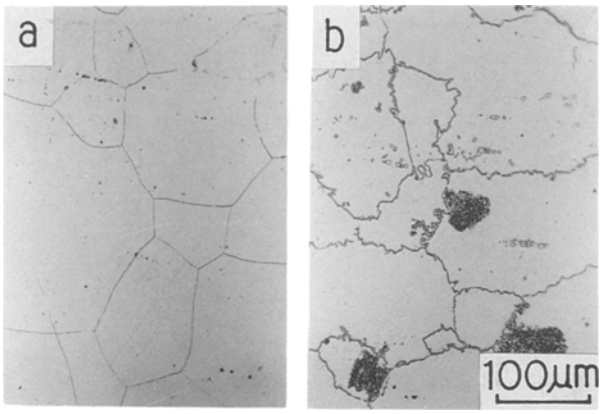

Figure 1 Optical micrographs of HS-21 alloys: (a) alloy N, 1250° C × 1 h → W.Q.; (b) alloy S, 1250° C × 1 h → F.C., 1050° C → W.Q. W.Q. = water quenched, F.C. = furnace cooled.)

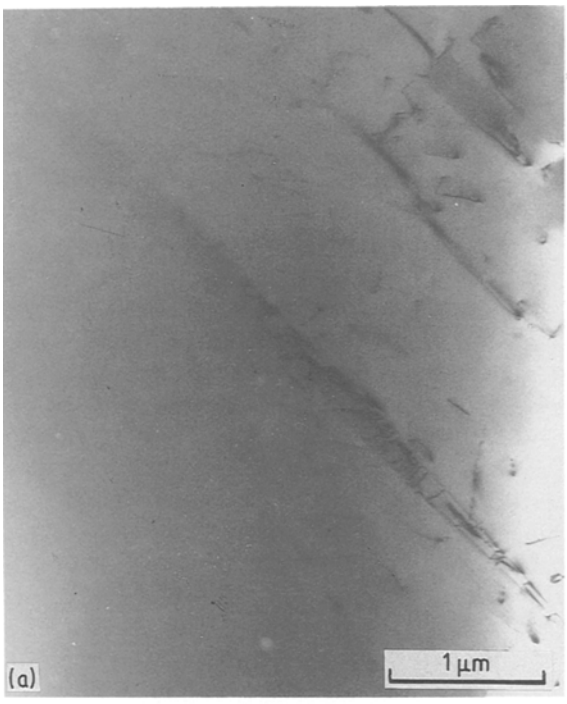

carbides (Fig. 2c). As reported in the previous paper [8], the crystallographic orientation of $M_{23}C_6$ carbides in the nodules was in parallel with that of the β-Co matrix (fcc) in the nodule, such that $(1\,1\,1)_{M_{23}C_6} \parallel (1\,1\,1)_{\beta\text{-Co}}$ and $(0\,\bar{1}\,1)_{M_{23}C_6} \parallel (0\,\bar{1}\,1)_{\beta\text{-Co}}$. The grain size of both specimens was the same and about 130 μm. The heat-treated specimens were machined to test pieces with 6 mm diameter and 30 mm gauge length for creep-rupture experiments.

Creep-rupture experiments were performed under more than three stress levels in the temperature range 816 to 1038° C (1500 to 1900° F) in air. The specimens were aged for 3 h at each test temperature to cause large amounts of matrix precipitates and were then loaded. The microstructure and fracture appearance of rupture specimens were examined by both optical and scanning electron microscopes. Specimens were electrolytically etched by 10% chromic acid in water before observations with the optical microscope. Transmission electron microscopy was also employed to identify the grain-boundary and matrix precipitates in these specimens.

3. Results and discussion

3.1. Effects of grain-boundary configuration on creep-rupture properties

Fig. 3 shows the rupture lives of HS-21 alloys at high temperatures. The rupture lives of specimens with serrated grain boundaries (alloy S) are considerably longer than those of specimens with straight grain boundaries (alloy N) under almost all test conditions. For example, the rupture life is about 145 h in alloy S under a stress of 137 MPa at 816° C, while it is about 57 h in alloy N under the same creep condition. The rupture lives of alloy S are more than twice as long as

Figure 2 Transmission electron micrographs of HS-21 alloys: (a) alloy N, (b) alloy S, (c) selected-area electron diffraction pattern of (b), $((1\,2\,3)_{\beta\text{-Co}} \parallel (1\,2\,3)_{M_{23}C_6})$.

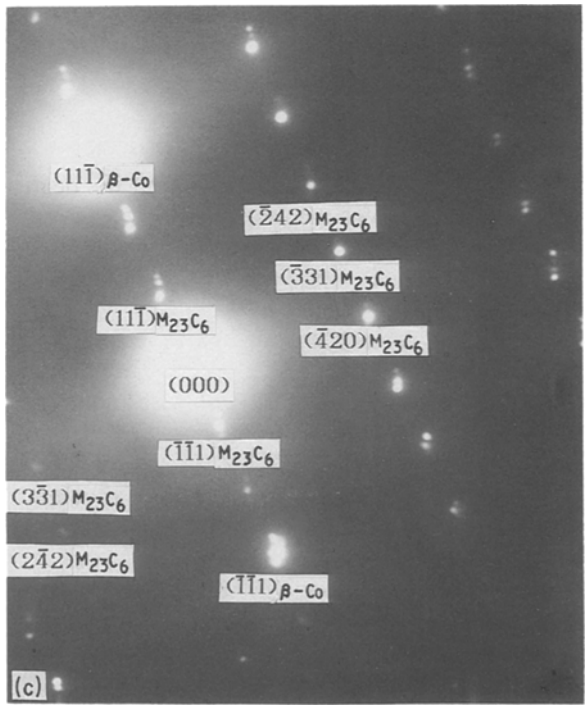

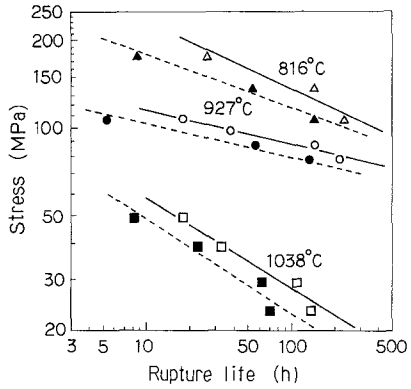

Figure 3 The rupture lives of HS-21 alloys at high temperatures: (△, ○, □) alloy S, (▲, ●, ■) alloy N.

those of alloy N even at temperatures above 927° C. Fig. 4 shows the creep ductility of HS-21 alloys. The rupture elongation is largely improved by serrated grain boundaries especially at lower temperatures. The increase of creep ductility by serrated grain boundaries is remarkable even at 1038° C.

Fig. 5 shows examples of creep curves in alloys S and N. The creep curves of HS-21 alloys in this study have a long tertiary creep regime and a very short steady-state creep regime in the temperature range from 816 to 1038° C, irrespective of grain-boundary configurations of specimens. It is obvious in this figure that alloy S has a larger creep ductility compared to alloy N. Fig. 6 shows the stress dependence of steady-state creep rate in these specimens. The stress dependence of steady-state creep rate changes with test temperature. The stress exponent decreases from about 6 to about 3 with increasing temperature, when a power law ($\dot{\varepsilon}_s \propto \sigma^n$, $\dot{\varepsilon}_s$ = steady-state creep rate, σ = stress, n = stress exponent) is applied. There is little difference between the steady-state creep rate of alloy S and that of alloy N under all the creep conditions. As will be seen later, $M_{23}C_6$ carbides precipitate in the matrix in both specimens and on grain boundaries in alloy N during holding and subsequent creep tests at each temperature. The experimental results mentioned above suggest that the strength of the matrix is almost the same in both specimens during creep.

Fig. 7 shows the creep rupture strength of HS-21 alloys. The rupture strength decreases with increasing temperature in both alloys S and N, but the decrease of rupture strength is smaller in alloy S than in alloy N. Alloy S has a higher rupture strength compared with alloy N even at 1038° C. Thus, the serrated grain

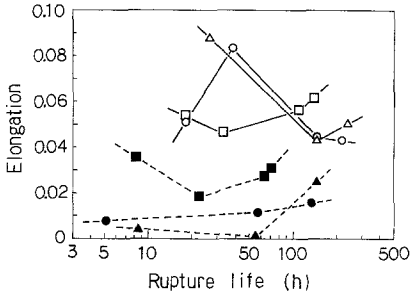

Figure 4 The creep ductility of HS-21 alloys at high temperatures: (△, ▲) 816° C, (○, ●) 927° C, (□, ■) 1038° C; open symbols, alloy S; solid symbols, alloy N.

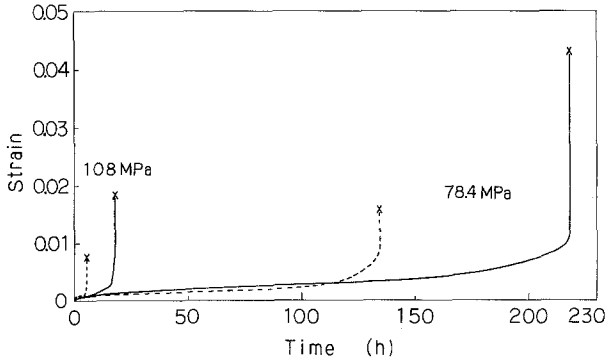

Figure 5 Creep curves of HS-21 alloys crept at 927° C: (——) alloy S, (– – –) alloy N.

boundary is effective in improving the rupture strength of HS-21 alloys at high temperatures.

It has been reported on nickel-based MAR M-200 alloys that directional solidification and mono-crystallization were able to increase rupture lives to twice or three times as long as those of conventional cast alloys with equiaxed grains under a stress of 30 000 psi (207 MPa) at 1800° F (982° C) [10, 11]. In this study, rupture lives of HS-21 alloys with serrated grain boundaries (alloy S) were about twice as long as those of the alloys with straight grain boundaries even at 1038° C, where the applied stress was in the range 23.5 to 49 MPa. The improvement in creep ductility by serrated grain boundaries was also remarkable at this temperature. Serrated grain boundaries can be produced by a simple heat treatment, while it requires a high cost to obtain directionary solidified or single-crystal structures in superalloys. Thus, a heat treatment to produce serrated grain boundaries can be a viable method in improving the high-temperature properties of superalloys.

3.2. Microstructures and fracture appearance of ruptured specimens

Fig. 8 shows microstructures and fracture surfaces of the specimen with serrated grain boundaries (alloy S)

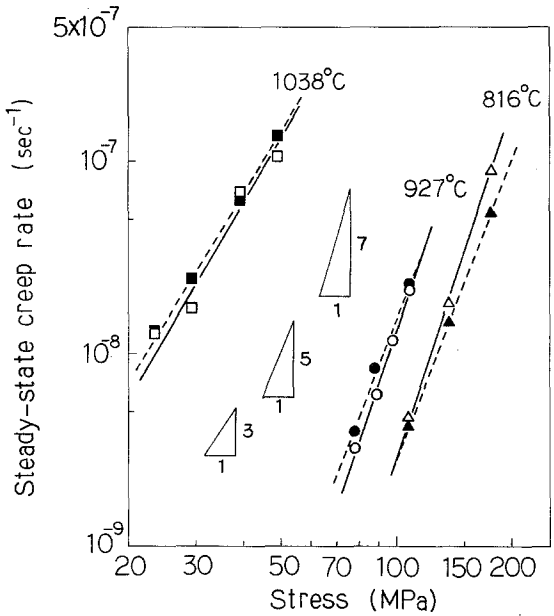

Figure 6 The stress dependence of steady-state creep rate in HS-21 alloys: (△, ○, □) alloy S, (▲, ●, ■) alloy N.

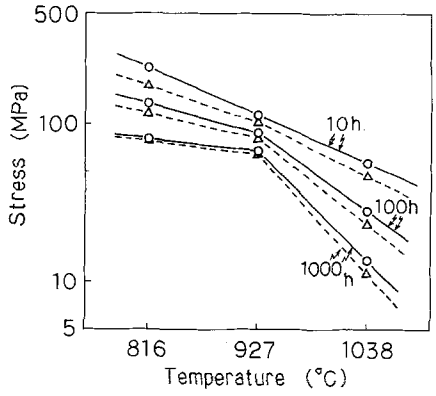

Figure 7 The temperature dependence of creep strength in HS-21 alloys: (○) alloy S, (△) alloy N.

and that with straight grain boundaries (alloy N) ruptured under a stress of 108 MPa at 816° C. The tensile direction is horizontal in the optical micrographs. Many microcracks can be observed on the grain boundaries near the fracture surface of both alloy S and alloy N (Figs 8a and b). Very fine matrix precipitates are formed on both specimens during creep. The fracture surface of alloy S consists of steps and ledges corresponding to serrated grain boundaries, and small dimples are also visible on the fracture surface (Fig. 8c), while the fracture surface of alloy N is typical of grain-boundary facets (Fig. 8d). The fracture appearances of these specimens at 927° C were almost the same as those at 816° C. Fig. 9 shows the microstructures and fracture surface of specimens ruptured under a stress of 29.4 MPa at 1038° C. Many microcracks and a fine dispersion of matrix precipitates is visible on both specimens (Figs 9a and b). Both fracture surfaces of alloy S and alloy N are covered with small dimples (Figs 9c and d). In alloy N (Fig. 9d) in particular, the fracture surface at this temperature is very different from that at 816° C (Fig. 8d). This indicates that the fracture mechanism changes with increasing temperature in alloy N. We have already reported that for austenitic 21Cr–4Ni–9Mn steels the mechanism of grain-boundary fracture initiation may have changed from triple-point cracking to other mechanisms due to the recovery by diffusion of atoms with increasing temperature during creep. The strengthening mechanism by serrated grain boundaries in creep can be related to the initiation and growth of grain-boundary cracks, because serrated grain boundaries are effective in inhibiting grain-boundary sliding, and thus in retarding the grain-boundary fracture. A study on fracture process in these alloys is now in progress.

Fig. 10 shows the matrix precipitates observed on alloys S and N ruptured under a stress of 108 MPa at 816° C. Very small precipitates are formed on grain boundaries of alloy N (Fig. 10a) and also in the matrix of both specimens (Figs 10a and b). These matrix precipitates, as well as the grain-boundary precipitates, are identified as $M_{23}C_6$ carbides which are in parallel orientation with the β-Co matrix (Fig. 10c). It is found that matrix $M_{23}C_6$ carbides dominantly precipitate on dislocations during ageing at 1000° C, while these matrix carbides precipitate on the stacking faults at 800° C [8]. These $M_{23}C_6$ carbides are considered to contribute to the strengthening of matrix during creep.

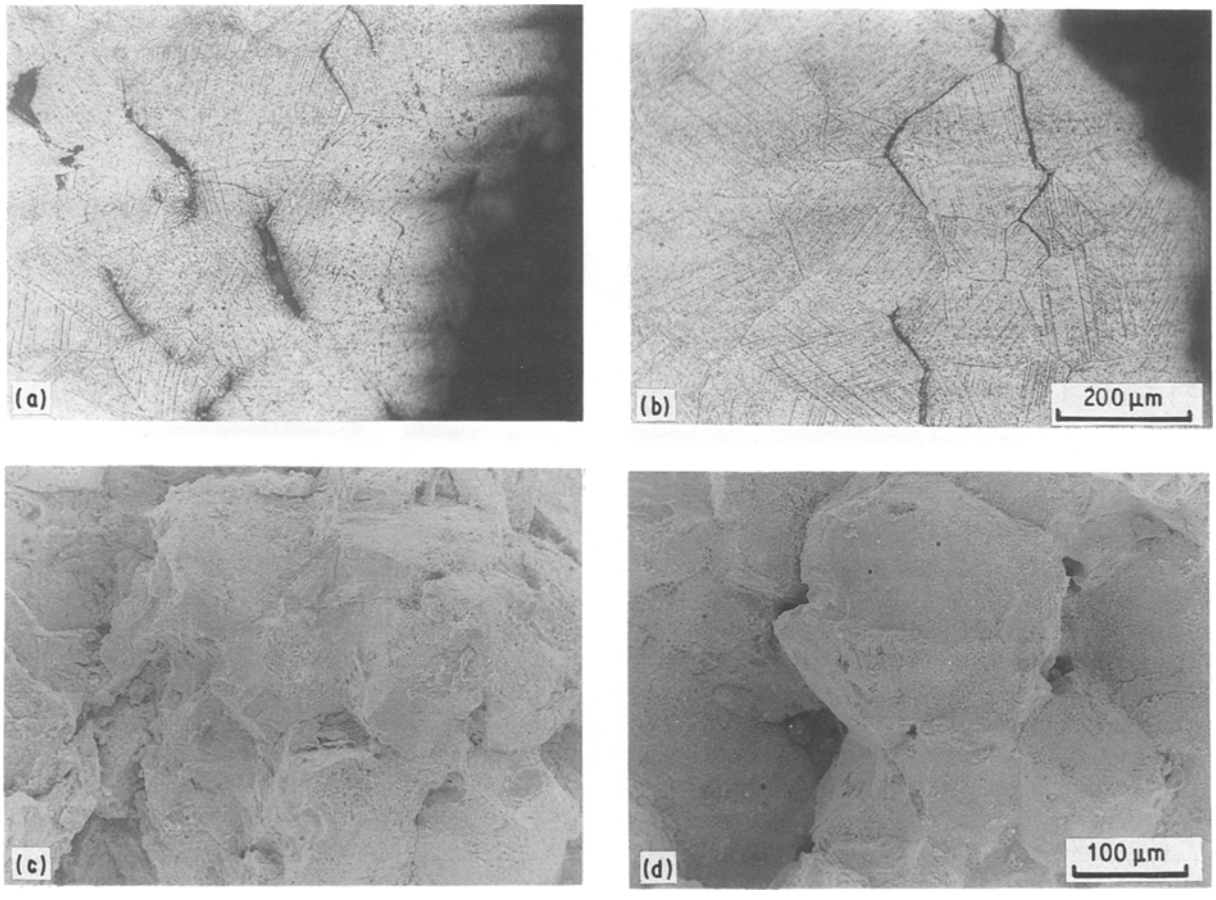

Figure 8 Microstructures and fracture surfaces of HS-21 alloys ruptured under a stress of 108 MPa at 816° C: (a, c) alloy S, (b, d) alloy N.

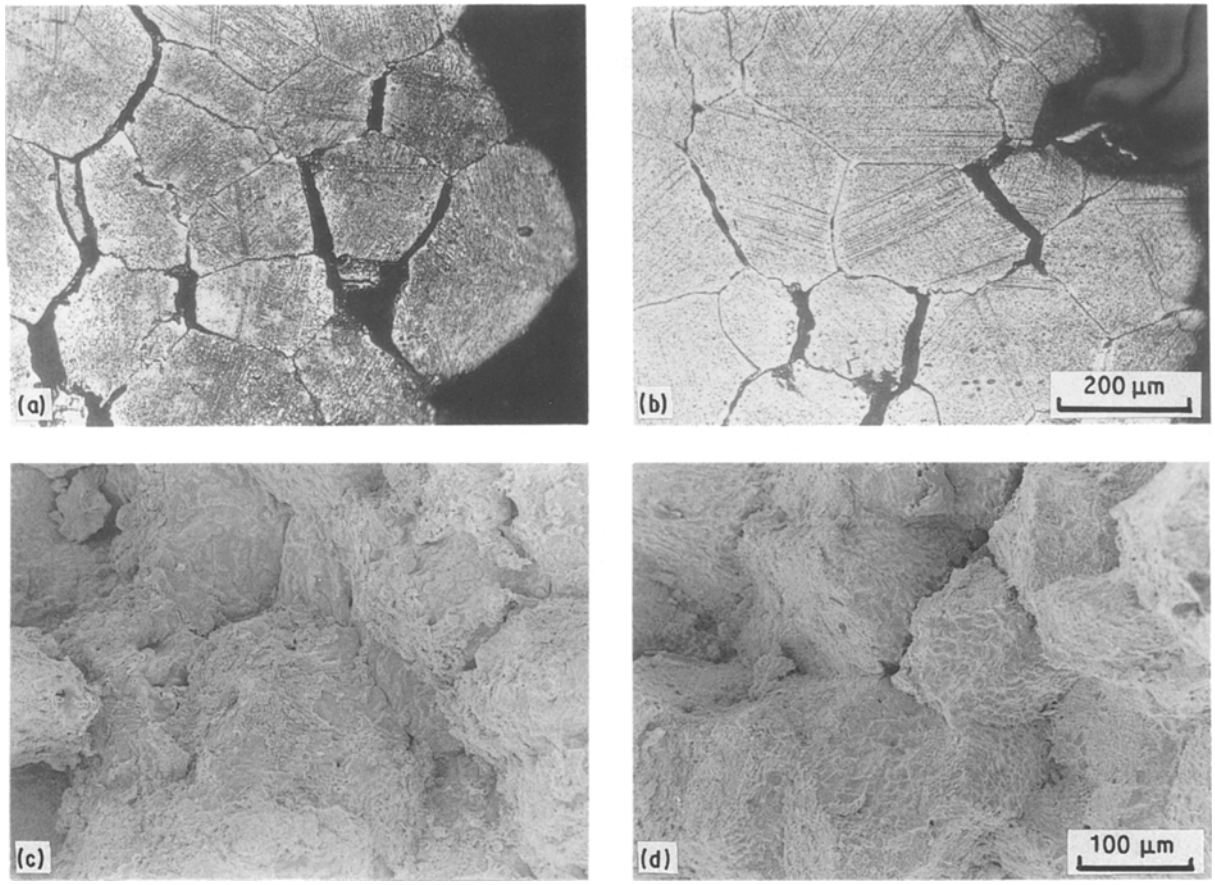

Figure 9 Microstructures and fracture surfaces of HS-21 alloys ruptured under a stress of 29.4 MPa at 1038° C.

4. Conclusions

The improvement of creep rupture properties by serrated grain boundaries was investigated using cobalt-based HS-21 alloys in the temperature range 816 to 1038° C (1500 to 1900° F). The following results were obtained.

1. Creep rupture properties of HS-21 alloys were considerably improved by serrated grain boundaries which were produced by a heat treatment. Rupture lives of specimens with serrated grain boundaries were more than twice as long as those of specimens with normal straight grain boundaries. The creep ductility of the alloys was also increased remarkably by serrated grain boundaries especially in the lower temperature range.

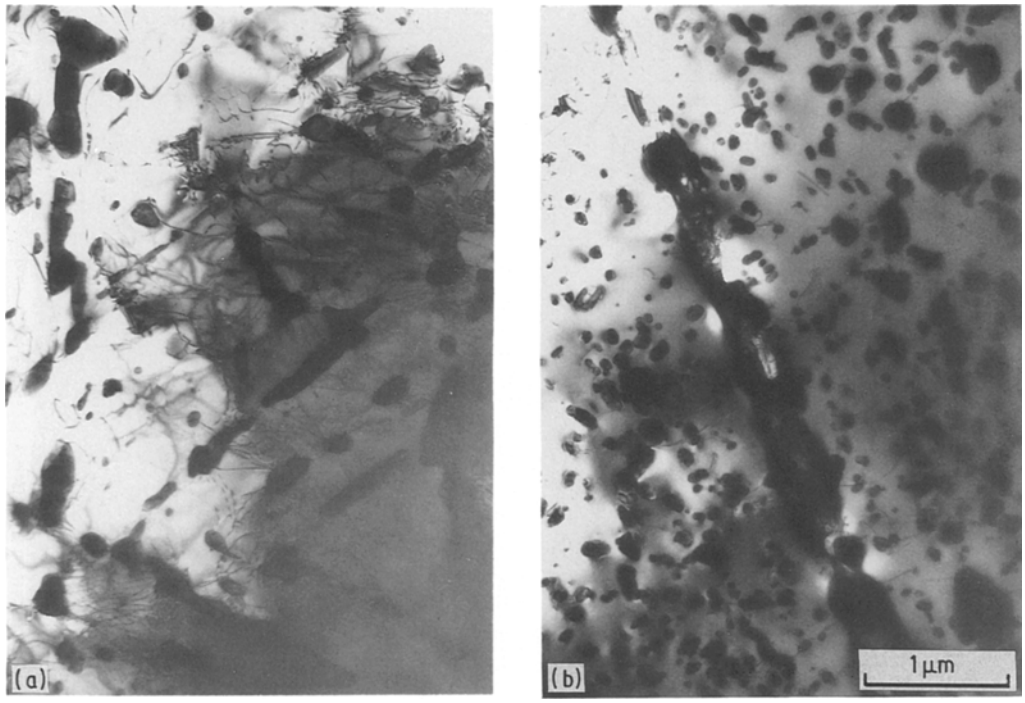

Figure 10 Transmission electron micrographs of HS-21 alloys ruptured under a stress of 137 MPa at 816° C: (a) alloy S, (b) alloy N, (c) selected-area electron diffraction pattern of (b), $((2\,1\,1)_{\beta\text{-Co}} \parallel (2\,1\,1)_{M_{23}C_6})$.

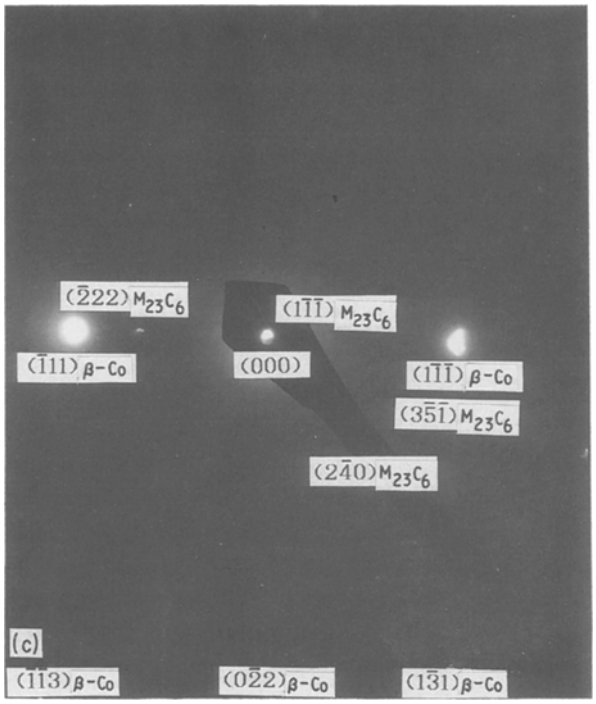

Figure 10 Continued.

2. The ductile grain-boundary fracture which contained small dimples, steps and ledges was observed on specimens with serrated grain boundaries, while typical grain-boundary facets prevailed in specimens with normal straight grain boundaries.

3. A simple heat treatment which developed serrated grain boundaries was a viable method in improving the creep-rupture properties of superalloys at high temperatures, while it would incur a much greater cost to obtain directionally solidified or single-crystal structures.

References

1. C. R. BROOKS, "Heat Treatment, Structure and Properties of Nonferrous Alloys" (American Society for Metals, Ohio, 1982) p. 229.
2. S. TAKADA and N. YUKAWA, *Bull. Jpn Inst. Met.* **6** (1967) 783.
3. C. YAKER and C. A. HOFFMAN, National Advisory Committee for Aeronautics, Technical Note 2320 (1951).
4. C. A. HOFFMAN and C. A. ROBARDS, *ibid.*, 2513 (1951).
5. N. J. GRANT and J. R. LANE, *Trans. ASM* **41** (1949) 95.
6. J. W. WEETON and R. A. SIGNORELLI, *ibid.* **47** (1955) 815.
7. R. N. TAYLOR and R. B. WATERHOUSE, *J. Mater. Sci.* **17** (1983) 3265.
8. H. IIZUKA and M. TANAKA, *ibid.* **21** (1986) 2803.
9. M. TANAKA, H. IIZUKA and F. ASHIHARA, *ibid.* **23** (1988).
10. B. H. KEAR and B. J. PIEARCEY, *Trans. AIME* **239** (1967) 1209.
11. F. L. VerSNYDER, R. B. BARROW, B. J. PIEARCEY and L. W. SINK, *Modern Castings* **55** (1969) 10.

Received 15 April
and accepted 7 September 1988